Thermodynamics of mRNA 5′ Cap Binding by Eukaryotic Translation Initiation Factor eIF4E†

Anna Niedzwiecka,‡,§ Edward Darzynkiewicz,‡ and Ryszard Stolarski*,‡

Department of Biophysics, Institute of Experimental Physics, Warsaw University, 02-089 Warszawa, Poland, and Biological Physics Group, Institute of Physics, Polish Academy of Sciences, 02-668 Warszawa, Poland

Received April 26, 2004; Revised Manuscript Received August 16, 2004

ABSTRACT: Translation of mRNA in eukaryotes begins with specific recognition of the 5′ cap structure by the highly conserved protein, eIF4E. The thermodynamics of eIF4E interaction with nine chemical cap analogues has been studied by means of emission spectroscopy. High-sensitivity measurements of intrinsic protein fluorescence quenching upon cap binding provided equilibrium association constants in the temperature range of 279 to 314 K. A van't Hoff analysis yielded the negative binding enthalpies for the entire cap analogue series, −16.6 to −81 kJ mol^{-1}, and the entropies covering the range of +40.3 to −136 J mol^{-1} K^{-1} at 293 K. The main enthalpic contributions come from interactions of the phosphate chains and positively charged amino acids and the cation−π stacking of 7-methylguanine with tryptophans. A nontrivial, statistically important isothermal enthalpy−entropy compensation has been detected (T_c = 399 ± 24 K), which points to significant fluctuations of *apo*-eIF4E and indicates that the cap-binding microstate lies 9.66 ± 1.7 kJ mol^{-1} below the mean energy of all available conformational states. For five cap analogues, large and positive heat capacity changes have been found. The values of $\Delta C_p°$ correlate with the free energies of eIF4E binding due to stiffening of the protein upon interaction with cap analogues. At biological temperatures, binding of the natural caps has both favorable enthalpy and favorable entropy. Thermodynamic coupling of cap-eIF4E association to intramolecular self-stacking of dinucleotide cap analogues strongly influences the enthalpies and entropies of the binding, but has a negligible effect on the resultant $\Delta G°$ and $\Delta C_p°$ values.

The 5′ termini of eukaryotic mRNAs as well as the uridine rich small nuclear RNAs (U snRNAs) synthesized in the nucleus by RNA polymerase II are cotranscriptionally modified to form the cap structure (*1*) consisting of 7-methylguanosine linked by a 5′-5′ triphosphate bridge to the first transcribed nucleoside (denoted m^{7}GpppN, or monomethylguanosine cap, MMG[1] cap, Chart 1). The MMG cap structure plays a pivotal role in several stages of gene expression which include promoting splicing of mRNA precursors (pre-mRNAs), facilitating RNA export to the cytoplasm, protecting mRNA against nucleolytic degradation, and stimulating protein synthesis (translation) (*2*). After nuclear export, the MMG cap of U snRNA is further methylated at the amino group to yield m$_3^{2,2,7}$GpppN (trimethylguanosine cap, TMG cap) (*3*), which serves as a targeting signal for import of small ribonucleoproteins (U snRNPs) back into the nucleus (*4*, *5*) where they take part in pre-mRNAs splicing (*6*). For their biological activities, the cap structures have to be properly recognized by the cap-binding proteins. There are several protein factors, e.g., cytoplasmic eukaryotic translation initiation factor 4E (eIF4E) (*7*) and nuclear cap binding complex (CBC) (*8*), which interact with the MMG cap. eIF4E is responsible for the control of initiation of protein translation, while CBC takes part in pre-mRNA splicing and nuclear export.

The eIF4E factor is to date the best biochemically (*9*) and biophysically (*10*−*16*) characterized cap binding protein. Nevertheless, the description of the detailed molecular mechanism of specific eIF4E−cap recognition still remains far from complete. eIF4E is a subunit of a larger complex, eIF4F, that also contains a scaffolding protein eIF4G and an RNA helicase, eIF4A (*17*). Following cap binding, eIF4F, in conjunction with eIF4B, unwinds the secondary structure of the mRNA, enabling recruitment of the ribosome to the translation start codon. Binding of eIF4E to the cap structure, which occurs during formation of the 48S initiation complex,

† This research was supported by the Polish Committee for Scientific Research (KBN 3 P04A 021 25, KBN PBZ 059/T09/10, BST 833/BF) and the Fogarty International Center, NIH (1 R03 TW006446).

* To whom correspondence should be addressed: Department of Biophysics, Institute of Experimental Physics, Warsaw University, 93 Zwirki & Wigury St., 02-089 Warszawa, Poland. E-mail: stolarsk@biogeo.uw.edu.pl. Tel: +48 22 55 40 772. Fax: +48 22 55 40 771.

‡ Warsaw University.

§ Polish Academy of Sciences.

[1] Abbreviations: eIF4E, eukaryotic initiation factor 4E and similarly 4F, 4G, 4A, 4B factors; CBC, nuclear cap binding complex; MMG, monomethylguanosine; TMP, trimethylguanosine; m^{7}G, 7-methylguanosine; m^{7}GMP, 7-methylguanosine 5′-monophosphate; m^{7}GDP, 7-methylguanosine 5′-diphosphate; m^{7}GTP, 7-methylguanosine 5′-triphosphate; m$_3^{2,2,7}$GTP, N^2,N^2,7-trimethylguanosine 5′-triphosphate; bz^{7}GTP, 7-benzylguanosine 5′-triphosphate; *p*-Cl-bz^{7}GTP, 7-(*p*-chlorobenzyl)guanosine 5′-trophosphate; m^{7}GpppG, P^1-7-methylguanosine-5′ P^3-guanosine-5′ triphosphate; m^{7}GpppC, P^1-7-methylguanosine-5′ P^3-cytidine-5′ triphosphate; m^{7}Gppppm^{7}G, P^1-7-methylguanosine-5′ P^3-7-methylguanosine-5′ tetraphosphate; HEPES, *N*-[2-hydroxyethyl]-piperazine-*N*′-[2-ethanesulfonic acid]; DTT, dithiothreitol; EDTA, disodium ethylenediaminetetraacetate.

10.1021/bi0491651 CCC: $27.50
Published on Web 09/30/2004

Chart 1: Structures of Cap Analogs Used in the Studies[a]

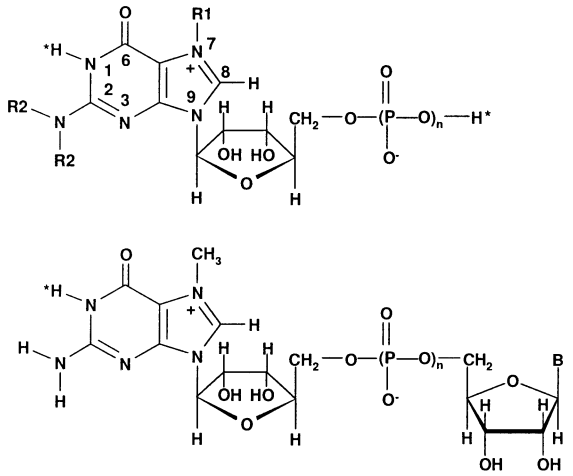

Cap analogue	R1	R2	n	B
m^7GMP	CH_3	H	1	--
m^7GDP	CH_3	H	2	--
m^7GTP	CH_3	H	3	--
bz^7GTP	CH_2-Φ	H	3	--
p-Cl-bz^7GTP	CH_2-Φ-Cl	H	3	--
$m_3^{2,2,7}$GTP	CH_3	CH_3	3	--
m^7GpppG	--	H	3	G
m^7GpppC	--	H	3	C
m^7Gppppm^{7}G	--	H	4	m^7G

[a] Φ denotes the phenyl ring; protons that partially dissociate at pH 7.2 are marked with an asterisk ($pK_a^{N(1)-H} \sim 7.24-7.54$, depending on R2, R3, and *n* (*44*); $pK_a^{phosph} \sim 6.1-6.5$, depending on *n* (*89*)).

is a rate-limiting step for translation initiation (*18*, *19*). eIF4E is present in the cell at much lower concentrations than other translation initiation factors (*20*), and hence its biological activity is regulated mainly by its cellular accessibility (*9*). Overexpression of eIF4E has a strong effect on cell growth and phenotype (*21*, *22*), since it causes accelerated cell division, malignant transformation, and inhibition of apoptosis (*18*). In most cancers, including breast, head-and-neck, and lung cancers, eIF4E overexpression occurs up to 30-fold (*21*). A search for drugs is needed that can lower the levels of eIF4E in all these cases. Highly specific, synthetic cap analogues might neutralize the consequences of the elevated eIF4E activity in tumor cells.

Recognition of the 5′ mRNA cap by eIF4E (Figure 1) is accomplished mainly by charge-related interactions inside the cap-binding center (*10*), and accompanied by coupled processes, i.e., partial protonation of cap at N(1), uptake of ~65 water molecules by the complex, and the protein conformational change(s) (*13*, *14*). The thermodynamic description of such an intricate process, with dominating electrostatic effects and involving tens of participants, is necessary to gain a deeper insight into the nature of the eIF4E−cap binding process, and can facilitate the search for new therapeutic agents that act at the level of fast and selective translational control.

In an effort to elucidate the structural features of the 5′ cap of mRNAs responsible for the eIF4E binding thermodynamics, we have performed spectroscopic studies on nine chemically altered cap analogues in solution. The aim of the present work was to explain the biological properties of the eIF4E activity in terms of quantitative thermodynamic parameters, i.e., standard molar enthalpy, entropy, and heat capacity changes. An accurate account of these properties is of importance in the context of the interplay between different proteins which bind to the mRNA 5′ cap in the cell. Moreover, a thorough description of formation of the eIF4E−cap complexes contributes to a more general model for protein−nucleic acid interactions. The unique nature of our system lies in the dominating role of the cation−π stacking in specific, intermolecular recognition and complex stabilization. This is important in the general context of scientific studies, since there is a noticeable tendency in the literature to focus thermodynamic investigations on uncharged, hydrophobic systems, while electrostatic interactions between macromolecules are routinely analyzed mainly with respect to ionic equilibria, without much attention to temperature-dependent effects. Thus, the work presented enriches the rather scant data in this still unexplored area of research.

MATERIALS AND METHODS

Chemical syntheses and purification of cap analogues (Chart 1) were performed as described previously (*23*). Expression of murine eIF4E (residues 28−217) was done without contact with cap (*13*, *24*). All other chemicals were of analytical grade, purchased from Sigma-Aldrich, Merck, Carl Roth (Germany), or Fluka (USA).

Fluorescence Measurements. Absorption and fluorescence spectra were recorded on Lambda 20 UV/VIS and LS-50B instruments (Perkin-Elmer Co., Norwalk, CT), in a quartz semimicro cuvette (Hellma, Germany) with a magnetic stirrer and optical lengths of 4 mm and 10 mm for absorption and emission, respectively. Titration experiments were performed in 50 mM HEPES/KOH pH 7.20, 100 mM KCl, 1 mM DTT, and 0.5 mM EDTA. Buffers of pH 7.20 (±0.01 unit) and constant ionic strength were adjusted independently for each temperature (Beckman Φ300 pH-meter, Germany). Solutions were passed through 0.22 μm pore size filters and degassed. Cap analogue concentration was obtained from weighed amounts (±5%) and checked spectrophotometrically (*25*). Only freshly prepared (not frozen) protein was used. Immediately before the spectroscopic measurements, the protein solution was filtered through a Millipore Ultrafree 0.5 mL Biomax 100 kDa NMWL and softly degassed. The total concentration of eIF4E was determined from absorbance (ϵ_{280} = 53900 cm^{-1} M^{-1}). The temperature was controlled with a thermocouple inside the thermostated cuvette (±0.2 °C). The excitation wavelength of 280 nm (slit 2.5 nm, auto cutoff filter) and the emission wavelength of 335, 336, or 337 nm (slit 2.5 to 4 nm, 290 nm cutoff filter) were applied, with an automatic correction for the photomultiplier sensitivity. The fluorescence intensity was monitored by registration of entire spectra (310 nm to 400 nm) and during continuous, time-synchronized titration at a single wavelength, with an integration time of 30 s and a gap of 30 s for addition of the ligand. During the gap, the UV xenon flash lamp was switched off to avoid photobleaching the sample. Titrations were performed at several eIF4E concentrations (40 nM to 0.5 μM), under steady-state conditions provided by preincubation in an appropriate buffer. Aliquots (1 μL) of increasing ligand concentrations (1 μM to 5 mM) were injected manually to 1400 μL of eIF4E solution. The fluorescence intensities were corrected for the *inner filter* effect (*26*) and for dilution (≤3.2%). At higher temperatures (~40 °C), protein fluorescence decreased with time due to partial thermal denaturation of eIF4E. A correction for a

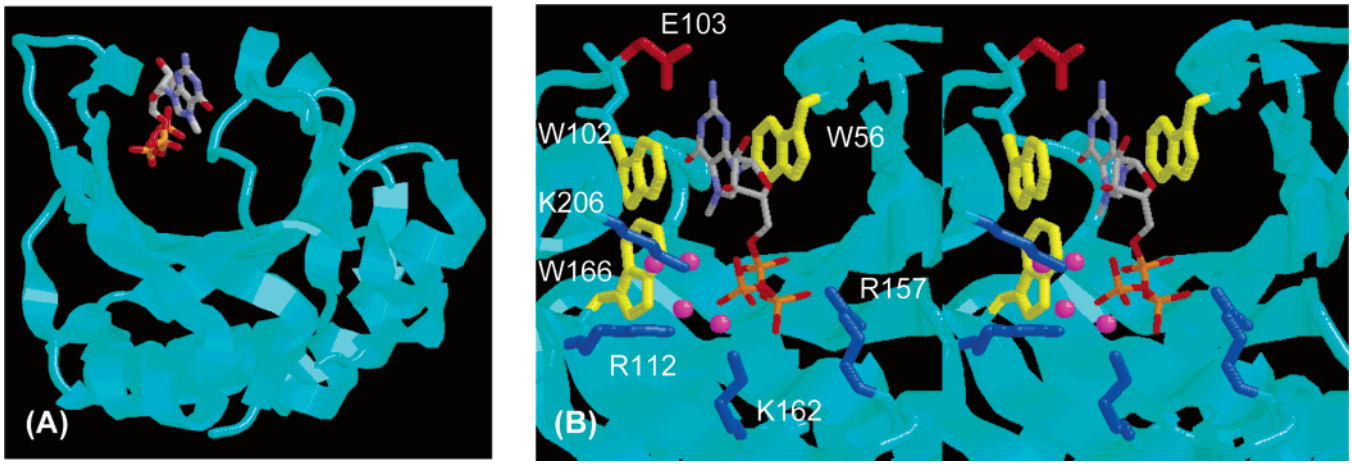

FIGURE 1: Three-dimensional structure of murine eIF4E (cyan) bound to m^{7}Gppp (thin sticks, CPK colors) determined by X-ray crystallography (PDB ID: 1L8B (*13*)). (A) General view of the eIF4E−m^{7}Gppp complex. (B) Stereoview of the cap-binding site; the key intermolecular contacts are shown, i.e., sandwich stacking of 7-methylguanine moiety between Trp102 and Trp56 (yellow thick sticks), hydrogen bonding with Glu103 (red thick sticks), and interactions of the phosphate chain by direct or water (magenta spheres) mediated hydrogen bonds or salt bridges with the basic amino acids (blue thick sticks).

fluorescence decrease as a function of time was applied to cancel the fluorescence changes that did not result from ligand binding. Monitoring of the fluorescence signal was continued for 10−20 min after termination of the titration. The exponential curve was fitted to the time-dependent data at the final ligand concentration, and the former titration data were then corrected. The latter two corrections had only a slight influence on the resulting K_{as} values (within 0.3 standard deviation) but improved the goodness of fit (R^2 and P value).

Fluorescence Data Analysis. The total protein concentration [P] is the sum of the active fraction [P_{act}] and the inactive [P_{inact}] fraction that does not interact with the ligand. The initial fluorescence intensity ($F(0)$) of the pure protein is equal to

$$F(0) = [P_{act}]\phi_{Pact-free} + [P_{inact}]\phi_{Pinact} \quad (1)$$

where ϕ is the fluorescence efficiency. The observed fluorescence intensity (F) after addition of the fluorescent ligand of $\phi_{lig-free}$ is given by

$$F = [P_{act}]_0\phi_{Pact-free} + [cx]f_{cx} + [L]_0 f_{lig-free} + [P_{inact}]\phi_{Pinact} \quad (2)$$

No assumptions regarding the fluorescence efficiency of the inactive protein are necessary.

The fluorescence intensity as a function of the total ligand concentration is expressed as

$$F = F(0) - [cx](\Delta\phi + \phi_{lig-free}) + [L]\phi_{lig-free} \quad (3)$$

where

$$[cx] = \frac{[L] + [P_{act}]}{2} + \frac{1 - \sqrt{(K_{as}([L] - [P_{act}]) + 1)^2 + 4K_{as}[P_{act}]}}{2K_{as}} \quad (4)$$

and $\Delta\phi = \phi_{Pact-free} - \phi_{cx}$ is the difference between the fluorescence efficiencies of the *apo*-protein and the complex. The theoretical curve (eqs 3 + 4) with the parameters K_{as}, [P_{act}], $\Delta\phi$, and $\phi_{lig-free}$ was fitted to the experimental data points. The latter parameter was independently verified experimentally (±4%).

Thermodynamics. The temperature dependence of K_{as} was analyzed according to the van't Hoff isobaric equation either in the nonlinear form (*27*),

$$\ln K_{as} = \frac{\Delta C_p^\circ}{R}\left[\frac{T_H}{T} - \ln\left(\frac{T_S}{T}\right) - 1\right] \quad (5)$$

or in the linear form,

$$\ln K_{as} = \frac{\Delta S^\circ}{R} - \frac{\Delta H^\circ}{RT} \quad (6)$$

(index "°" refers to the pseudostandard state at concentrations of 1 mol/L, i.e., unit molarity, R is the gas constant, and T is the absolute temperature). In the former case, the molar heat capacity change (ΔC_p°) and the characteristic temperatures (T_S where $\Delta S^\circ = 0$, and T_H where $\Delta H^\circ = 0$) were obtained as free parameters of the fitting. The molar entropy (ΔS°) and enthalpy (ΔH°) changes were calculated as

$$\Delta S^\circ = \Delta C_p^\circ \ln\left(\frac{T}{T_S}\right) \quad (7)$$

$$\Delta H^\circ = \Delta C_p^\circ (T - T_H) \quad (8)$$

In the latter case, the constant values of ΔS° and ΔH° were fitted. The molar Gibbs free energy of binding (ΔG°) was calculated as

$$\Delta G^\circ = -RT \ln K_{as} \quad (9)$$

where the binding constants (K_{as}) were used for asymmetrical dinucleotide and mononucleotide cap analogues, and the microscopic binding constants ($K_{as}^{(micro)} = 0.5K_{as}$) were used for m^{7}Gppppm^{7}G because of entropic effects.

NMR Spectroscopy. ^{1}H NMR spectra of *N*-acetyltryptophanamide and m^{7}GMP were recorded on a VarianUNITY-plus 500 MHz spectrometer, in 1/15 M phosphate buffer, pH 5.6 or 5.2, with sodium 3-trimethylsilyl-[2,2,3,3-$^2H_4$]-propionate (TSP) as internal standard, and 10% ^2H_2O for

spin locking. A binominal 1331 experiment was used for water suppression (*28*). The proton assignments were made on the basis of the splitting patterns and the values of chemical shifts (±0.001 ppm). The unambiguous assignment for the H(4)/H(7) and H(5)/H(6) proton pairs in the tryptophan indole ring were derived from analyses of the cross peaks in the 2D ROESY spectrum (*29*). The observed changes of ^{1}H chemical shifts ($\Delta\delta = \delta$(mixture) − δ(free)) of tryptophan at a concentration of c_{trp} due to stacking with m^{7}GMP at 298 K depend on the total cap analogue concentration (c_{cap}),

$$\Delta\delta = \Delta\delta_{st}\left(1 - \frac{c_u}{c_{trp}}\right) \tag{10}$$

where $\Delta\delta_{st}$ is the maximal change of the chemical shift for the stacked proton (fitted as a free parameter), and the equilibrium concentration of the unbound proton (c_u) is related to a fitted association constant (K):

$$c_u = \frac{(c_{trp} - c_{cap})}{2} + \frac{\sqrt{K^2(c_{trp} - c_{cap})^2 + 2K(c_{trp} + c_{cap}) + 1} - 1}{2K} \tag{11}$$

Temperature dependence of the observed differences of ^{1}H chemical shifts of tryptophan at 1 mM in the presence of 29.8 mM m^{7}GMP is described as $\Delta\delta$ as defined above, but the association constant depends on T according to the van't Hoff equation, with $\Delta S°$ and $\Delta H°$ either fitted as constant parameters or treated as functions of temperature (eqs 7, 8):

$$K = \exp\left(\frac{\Delta S°}{R} - \frac{\Delta H°}{RT}\right) \tag{12}$$

Computer simulations of relative orientation of two heteroaromatic rings were performed on the basis of NMR data with aid of the GEOSHIFT program (*30*).

Coupling between Binding and Conformational Transition of the Ligand. Thermodynamic parameters describing intramolecular base stacking of dinucleotide cap-analogues in the cationic form, i.e., entropy ($_1\Delta S°$) and enthalpy ($_1\Delta H°$) changes (*31*), were used to calculate stacking/unstacking equilibrium constants ($_1K$), contributions to enthalpy ($\Delta H°_{sst}$), entropy ($\Delta S°_{sst}$), and heat capacity ($\Delta C_p°_{sst}$) changes, which result from an induced shift in the self-stacking equilibrium, and intrinsic enthalpy ($\Delta H°_0$) and entropy ($\Delta S°_0$) changes of the cap−eIF4E association, according to the equations for mandatory coupling of cap self-stacking to cap−eIF4E binding (*32*):

$$_1K = \exp\left(\frac{_1\Delta S°}{R} - \frac{_1\Delta H°}{RT}\right) \tag{13}$$

$$\Delta H°_{sst} = -\frac{_1\Delta H°(_1K)}{1 + _1K} \tag{14}$$

$$\Delta S°_{sst} = -R\ln(1 + _1K) - \frac{_1\Delta H°(_1K)}{T(1 + _1K)} \tag{15}$$

$$\Delta C_p°_{sst} = -\frac{(_1\Delta H°)^2\,_1K}{RT^2(1 + _1K)^2} \tag{16}$$

$$\Delta H°_0 = \Delta H° - \Delta H°_{sst} \tag{17}$$

$$\Delta S°_0 = \Delta S° - \Delta S°_{sst} \tag{18}$$

Statistical analysis was carried out on the basis of the runs test and the P value (*33*). Goodness of fits of binding isotherms (R^2) was ≥0.999. Other R^2 values are provided in the text. Discrimination between two models of different numbers of degrees of freedom (ν_1 and ν_2) was based on the Snedecor's F-test (*33*), with the significance level of $P(\nu_1, \nu_2) < 0.1$ or < 0.05. Errors (one standard deviation) were calculated according to the propagation rules (*34*). Isothermal enthalpy−entropy compensation was analyzed including uncertainties of both $\Delta H°$ and $\Delta S°$. Regressions were performed by means of the linear or nonlinear, least-squares method, using PRISM 3.02 from GraphPad Software Inc. or ORIGIN 6.0 from Microcal Software Inc.

RESULTS

To obtain values of equilibrium association constants (K_{as}) for eight structurally altered mRNA 5′ cap analogues, m^{7}GMP, m^{7}GDP, m^{7}GTP, m$_3^{2,2,7}$GTP, bz^{7}GTP, *p*-Cl-bz^{7}GTP, m^{7}GpppC, and m^{7}Gppppm^{7}G (Chart 1), fluorescence titration experiments were performed in the temperature range of 279−314 K. Examples of binding isotherms for eIF4E association with m^{7}GpppC at selected temperatures are presented in Figure 2. The results allowed us to derive the thermodynamic parameters describing formation of the complexes.

Van't Hoff Analysis of eIF4E Binding to Cap Analogues. Standard molar enthalpy changes ($\Delta H°$), entropy changes ($\Delta S°$), and the corresponding Gibbs free energies for the formation of the complexes ($\Delta G°$) at 293 K determined from the van't Hoff dependencies are collected in Table 1. Generally, the association of eIF4E with the mRNA 5′ cap at 273 K results from a favorable enthalpy change for the entire series of the cap analogues, and is related to either unfavorable or favorable entropy change, depending on the cap analogue. The cap analogues of the highest affinity ($\Delta G°$) for eIF4E have the most negative enthalpy of association, from −50 to −81 kJ mol^{-1}, while for the ligands of lower affinity $\Delta H°$ is −17 to −36 kJ mol^{-1}. The binding entropy ranges from +40 to −136 J mol^{-1} K^{-1}. One exception among the most tightly binding analogues is *p*-Cl-bz^{7}GTP, which has a small binding enthalpy of only −38.5 kJ mol^{-1} but a large positive binding entropy of +16.7 J mol^{-1} K^{-1}.

Heat Capacity Changes. The linear character of the van't Hoff plots is lost for the analogues of moderate affinity for eIF4E (Figure 3). The thermodynamic parameters that are related to the nonlinearity, i.e., standard molar heat capacity change under constant pressure ($\Delta C_p°$), and the critical temperatures where $\Delta H° = 0$ and $\Delta S° = 0$ (T_H and T_S, respectively) are assembled in Table 2. The large $\Delta C_p°$ values resulting from the nonlinearity are surprisingly positive, from +1.66 for m^{7}Gppppm^{7}G up to +5.12 kJ mol^{-1} K^{-1} for the m$_3^{2,2,7}$GTP−eIF4E association, and T_H is higher than T_S. The results derived from the nonlinear fitting are statistically unambiguously superior to those derived from the linear one

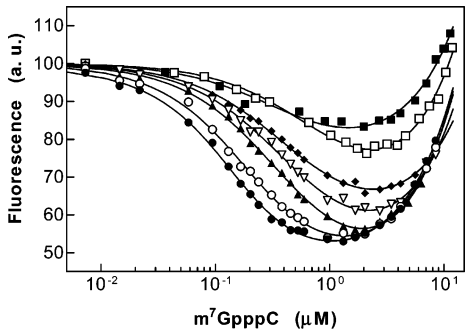

FIGURE 2: Binding isotherms for eIF4E interaction with m^{7}GpppC at different temperatures: 280.0 (●), 287.4 (○), 292.8 (▲), 299.4 (▽), 304.0 (◆), 308.6 (□), 313.1 (■). Intrinsic eIF4E fluorescence is quenched upon titration with the cap analogue. Increasing fluorescence intensity at higher cap analogue concentrations originates from the free ligand in solution. Titrations were performed in 50 mM HEPES/KOH (pH 7.2), 100 mM KCl, 1 mM DTT, and 0.5 mM EDTA.

Table 1: Standard Molar Enthalpy Changes ($\Delta H°$) and Entropy Changes ($\Delta S°$) Obtained from the van't Hoff Isobaric Equation for Binding of eIF4E to mRNA 5′ Cap Analogues, and Standard Molar Gibbs Free Energy Changes ($\Delta G°$) Calculated from the Association Constants, at 293 K, pH 7.2

cap analogue	$\Delta H°$ (kJ mol^{-1})	$\Delta S°$ (J mol^{-1} K^{-1})	$\Delta G°$ (kJ mol^{-1})
m^{7}GMP[a]	-36.0 ± 7.9	-9.3 ± 3.4	-33.15 ± 0.20
m^{7}GDP[b]	-61.9 ± 2.9	-69.8 ± 10.5	-41.031 ± 0.179
m^{7}GTP[b]	-74.3 ± 3.6	-98.7 ± 12.1	-45.109 ± 0.090
bz^{7}GTP[b]	-56.5 ± 3.8	-52.7 ± 13.0	-40.669 ± 0.060
p-Cl-bz^{7}GTP[b]	-38.5 ± 4.6	$+16.7 \pm 15.5$	-42.94 ± 0.21
m$_3^{2,2,7}$GTP[a]	-16.6 ± 2.5	$+40.3 \pm 12.7$	-28.94 ± 1.36
m^{7}Gppppm^{7}G[a,c]	-81 ± 54	-136 ± 88	-41.377 ± 0.146
m^{7}GpppG[a,d]	-65 ± 31	-91 ± 58	-38.555 ± 0.152
m^{7}GpppC[a]	-50 ± 28	-45 ± 29	-36.42 ± 0.40

[a] Temperature-dependent $\Delta H°$ and $\Delta S°$ (nonlinear van't Hoff plot). [b] Constant $\Delta H°$ and $\Delta S°$ (deviation of van't Hoff plot from linearity not detected). [c] The microscopic association constant ($K_{as}^{micro} = 0.5\ K_{as}$) has been taken into account. [d] Data from ref *14*.

at the significance level (*P*) resulting from the Snedecor's *F*-test, from 0.049 to even less than 0.0001. Involvement of the next fitting parameter that would be related to a possible temperature dependence of $\Delta C_p°$ did not provide further improvement of the results. These results appeared questionable in light of considerable data (e.g., refs *35*−*39*) reporting negative $\Delta C_p°$ values for protein−ligand interactions. For this reason we confirmed independently the van't Hoff parameters for eIF4E binding to m^{7}GpppG by direct isothermal microcalorimetric measurements of temperature-dependent enthalpy changes; this yielded $\Delta C_p°_{cal} = +1.94 \pm 0.06$ kJ mol^{-1} K^{-1} (*14*).

Due to the nonzero $\Delta C_p°$, which is large in comparison with $\Delta S°$, temperature-dependent enthalpy−entropy compensation (*37*) occurs (Figure 4). Binding of eIF4E to the cap analogues is characterized by both favorable enthalpy and favorable entropy between the characteristic temperatures T_S and T_H (Table 2). The stabilization of the complexes is efficient even though the $\Delta G°$ function attains its maximum at T_S; e.g., for the two analogues m^{7}GpppG (*14*) and m^{7}GpppC, which frequently occur as natural mRNA 5′ termini, the maximal values are about -38 kJ mol^{-1}.

Tryptophan Stacking with the Cationic 7-Methylguanosine Moiety. Searching for sources of the nonzero heat capacity changes, we investigated the possibility that the positive values of $\Delta C_p°$ could partially arise from stacking of tryptophan with the nontypical 7-methylguanosine cation. Stacking of $\pi-\pi$ type between nucleobases upon single helix formation is known to result in no heat capacity changes (*40*, *41*). As opposed to the regular, dispersive $\pi-\pi$ interactions, cation$-\pi$ stacking is due mainly to Coulombic attraction between the cation and the induced quadrupole charge distribution on the aromatic ring (*42*). To obtain thermodynamic information about pure cation$-\pi$ stacking, NMR spectroscopy was applied to examine the model system of 7-methylGMP and *N*-acetyltryptophanamide. Stacking between 7-methylG and tryptophan shifts the ^{1}H signals upfield (Figure 5A), yielding microscopic equilibrium association constants (*K*) for all protons of the order of magnitude of 10 M^{-1} at 298 K (Table 3). Very similar *K* values for the individual tryptophan protons point to a simple two-state model, in which the tryptophan−m^{7}GMP complex is in dynamic equilibrium with the separate molecules. Computer simulations of the changes of the tryptophan chemical shifts by means of the GEOSHIFT program (*30*) revealed parallel orientation of the stacked rings of tryptophan and m^{7}GMP, as opposed to other complexes of cap analogues with a short, tryptophan containing peptide, for which both parallel and perpendicular geometries were found (*43*).

Although stacking of tryptophan with the m^{7}GMP cation is a hydrophobic interaction, the binding is characterized by favorable enthalpy change and unfavorable entropy change, as determined on the basis of the temperature-dependent differences of ^{1}H chemical shifts of the tryptophan protons (Figure 5B). Satisfactory goodness of fit in terms of the sum-of-squares of deviations (R^2) is obtained assuming constant values of the enthalpy and entropy changes. For all tryptophan protons, they converge to the values of about -26 kJ mol^{-1} and -64 J mol^{-1} K^{-1}, respectively (Table 3). However, the *P*-value that refers to the proper distribution of fitting residuals is improved if a nonzero $\Delta C_p°$ value is allowed (Figure 5C). The heat capacity change thus estimated for cation$-\pi$ stacking is positive and quite substantial, up to $+0.4$ kJ mol^{-1} K^{-1}, which is rather a unique result.

Coupling of Other Equilibria to eIF4E−*Cap Binding*. Association of eIF4E with the 5′ terminus of the mRNA is mandatory coupled (*32*) to intramolecular self-stacking of the dinucleotide cap, since only the unstacked form can penetrate the eIF4E cap-binding slot. The question that arises is to what extent this coupling influences interaction with eIF4E (*44*). The values of self-stacking equilibrium constants ($_1K$), standard molar enthalpy changes ($_1\Delta H°$), the enthalpic ($\Delta H°_{sst}$) and entropic ($\Delta S°_{sst}$) contributions, and the apparent molar heat capacity changes ($\Delta C_p°_{sst}$) resulting from an induced shift in the conformational equilibrium of the cap upon binding to eIF4E at pH 7.2 have been determined (Table 4). Both $\Delta H°_{sst}$ and $\Delta S°_{sst}$ for each dinucleotide, m^{7}GpppG, m^{7}GpppC, and m^{7}Gppppm^{7}G, are positive and relatively large. They shift the negative values of the intrinsic thermodynamic parameters ($\Delta H°_0$, $\Delta S°_0$, Table 5) to the less negative values of the observed $\Delta H°$ and $\Delta S°$ (Table 1). While enthalpy and entropy changes of eIF4E binding to the dinucleotides are strongly affected by coupling with unstacking of the dinucleotides, the intrinsic binding free energies for the unstacked caps ($\Delta G°_0$, Table 5) are unaf-

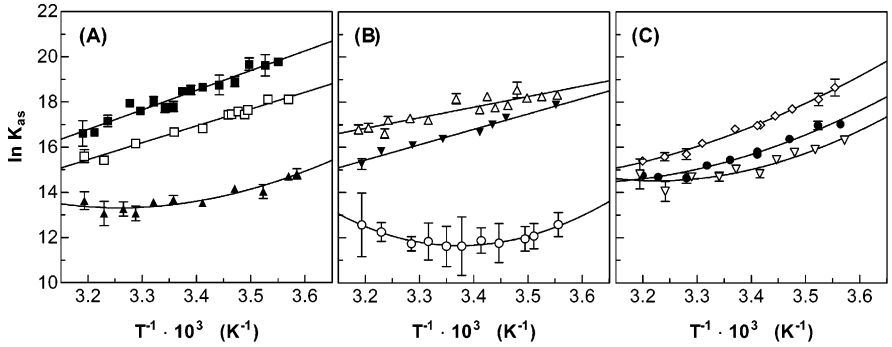

FIGURE 3: Dependence of van't Hoff plots for eIF4E−cap binding on structural alterations of the cap analogue: (A) elongation of the phosphate chain, m^7GMP (▲), m^7GDP (□), m^7GTP (■); (B) replacement of the 7-methyl group for larger substituents and dimethylation of 2-amino group, *p*-Cl-bz^{7}GTP (△), bz^{7}GTP (▼), $m_3^{2,2,7}$GTP (○); (C) change of the second base and number of the phosphate groups m^7Gppppm^{7}G (◇), m^7GpppG (●, (*14*)), m^7GpppC (▽).

Table 2: Critical Temperatures T_H (Where $\Delta H° = 0$), T_S ($\Delta S° = 0$), and Standard Molar Heat Capacity Changes under Constant Pressure ($\Delta C_p°$) Obtained from the Nonlinear van't Hoff Equation for mRNA 5′ Cap Analogues, at pH 7.2. Relative Decrease in Sum-of-Squares (F) in Comparison with That for the Linear Model, and the Probability of Random Improvement of Goodness of Fit $P(\nu_1, \nu_2)$. Calculated Gibbs Free Energies at T_S, $\Delta G°_{T_S} = \Delta H°_{T_S}$, and at T_H, $\Delta G°_{T_H} = -T_H \Delta S°_{T_H}$

cap analogue	T_H (K)	T_S (K)	$\Delta C_p°$ (kJ mol^{-1} K^{-1})	F	$P(\nu_1, \nu_2)$	$\Delta G°_{T_S}$ (kJ mol^{-1})	$\Delta G°_{T_H}$ (kJ mol^{-1})
m^7Gpppp(m^7G)[a]	342.0 ± 16.0	318.0 ± 7.8	+1.66 ± 0.57	8.54	0.019	−42 ± 32	−43.2 ± 5.3
m^7GpppG[b]	327.1 ± 15.2	307.4 ± 6.0	+1.92 ± 0.93	6.36	0.040	−38 ± 36	−39.0 ± 6.8
m^7GpppC	310.0 ± 6.2	297.6 ± 2.1	+2.96 ± 1.25	5.65	0.049	−37 ± 25	−37 ± 17
m^7GMP	306.9 ± 4.8	294.20 ± 1.68	+2.62 ± 0.97	7.34	0.027	−33 ± 18	−33.97 ± 0.84
$m_3^{2,2,7}$GTP	296.41 ± 0.43	290.86 ± 0.69	+5.12 ± 0.48	115	<0.0001	−28.4 ± 4.9	−29 ± 19

[a] Microscopic association constant has been taken into account. [b] Data from ref *14*.

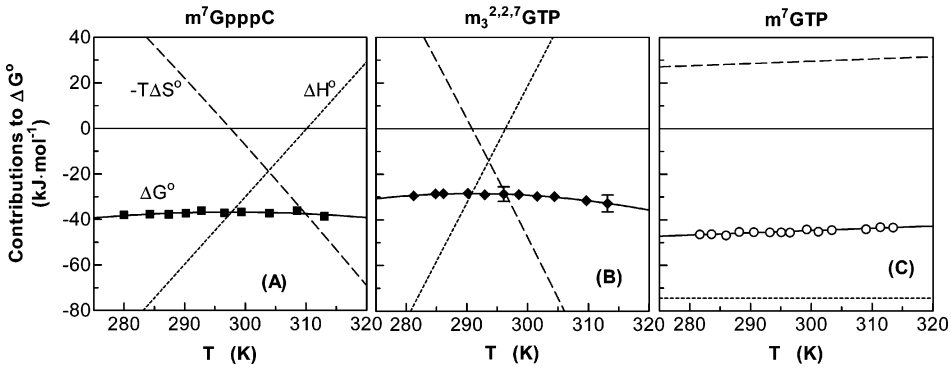

FIGURE 4: Temperature-dependent enthalpy−entropy compensation that accompanies the binding of m^7GpppC and $m_3^{2,2,7}$GTP to eIF4E. Theoretical nonlinear fit (—) to the binding free energies $\Delta G°$ (■ and ◆, respectively), the entropic (− − −), and enthalpic (···) contributions to $\Delta G°$ are plotted as a function of temperature. $\Delta S° = 0$ at T_S, and $\Delta H° = 0$ at T_H. Linear contributions to $\Delta G°$ of m^7GTP (○) are shown for comparison.

fected in comparison with the resultant $\Delta G°$ values (Table 1) due to very weak self-stacking equilibrium constants ($_1K$).

The $\Delta C_p°_{sst}$ contributions to the resultant heat capacity changes are negative, from −26 to −93 J mol^{-1} K^{-1} for the three analogues (Table 4), and negligibly shift the heat capacity changes of the overall association from the intrinsic values for the unstacked caps ($\Delta C_p°_0$, Table 5) to the resultant values ($\Delta C_p°$, Table 2).

Isothermal Enthalpy−Entropy Compensation in Congener Series. The enthalpic and entropic contributions to the Gibbs free energies of eIF4E binding to the series of cap analogues at 293.16 K (Table 1) appear to satisfy a linear relationship with the high correlation coefficient $R^2 = 0.975$ (Figure 6). The slope yields the compensation temperature $T_c = 399 \pm 24$ K. The result is exactly the same, irrespective of the data set chosen for the dinucleotide cap analogues, i.e., either the intrinsic ($\Delta H°_0$, $\Delta S°_0$, Table 5) or observed ($\Delta H°$, $\Delta S°$, Table 1) parameters. Hence, although the resultant enthalpy and entropy of interaction are significantly influenced by self-stacking, the general thermodynamic properties of recognition of the mRNA 5′ cap by eIF4E are insensitive to it.

Enthalpy−entropy compensation is a widely reported phenomenon, often considered an extra-thermodynamic feature of complex molecular systems in which molecules fluctuate or interact with the aqueous medium. However, several detailed and critical reviews of compensation in congener series have appeared, demonstrating that it is in most cases a trivial observation or an artifact that follows immediately from applied experimental conditions (*45*−*47*). There are three categories of trivial compensation (*47*). (1) When the congeners differ simply in the number or size of similar substituents, the compensation results from the presence of a single source of additivity. The series of cap analogues studied here contains several distinct sources of additivity: phosphate groups at the ribose ring, methyl

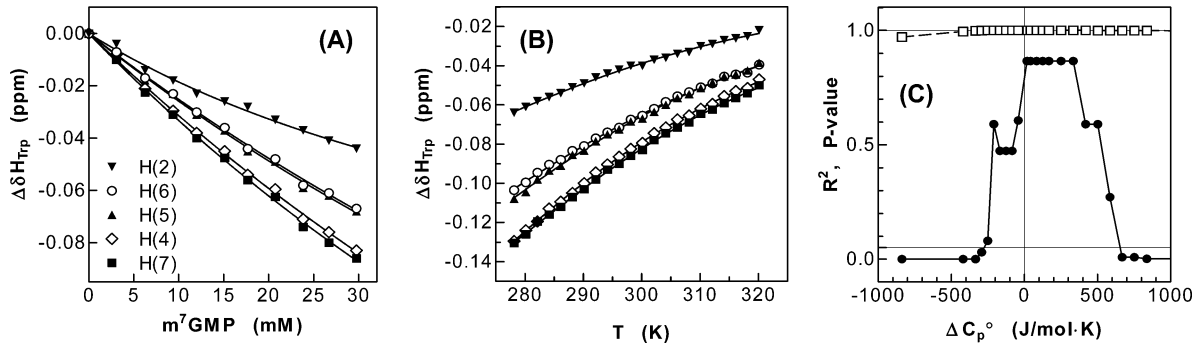

FIGURE 5: (A) Changes of ^{1}H chemical shifts of *N*-acetyltryptophanamide at 1 mM due to stacking with the 7-methylguanine moiety upon titration with m^{7}GMP at pH 5.6, 298 K. (B) Temperature dependence of changes of ^{1}H chemical shifts of *N*-acetyltryptophanamide at 1 mM in the presence of 29.8 mM m^{7}GMP at pH 5.6. (C) Goodness of fit (R^2, □) and probability of random distribution of fitting residuals (*P*-value, ●) for the curve fitted to temperature-dependent changes of the H(7) proton chemical shifts (Δδ H(7)) related to *N*-acetyltryptophanamide stacking with m^{7}GMP at pH 5.6 with the fixed ΔC_p° values indicated in the figure.

Table 3: Microscopic Equilibrium Association Constants for Tryptophan Protons Related to Stacking of *N*-Acetyltryptophanamide with m^{7}GMP at pH 5.6, 298 K, and van't Hoff Enthalpy (ΔH°) and Entropy (ΔS°) Changes, Fitted as Constant Parameters

protons	K (M^{-1})	ΔH° (kJ mol^{-1})	ΔS° (J mol^{-1} K^{-1})
H(2)	15.9 ± 3.8	−26.6 ± 1.8	−65.8 ± 4.6
H(4)	6.5 ± 1.6	−25.87 ± 0.78	−64.0 ± 1.9
H(5)	6.7 ± 2.0	−26.3 ± 1.4	−65.1 ± 3.4
H(6)	5.9 ± 1.8	−25.7 ± 1.1	−62.4 ± 2.7
H(7)	7.8 ± 1.3	−26.44 ± 0.79	−64.1 ± 2.0

substituents at the exocyclic 2-amino group of the 7-methylguanine moiety, different aromatic substituents for the 7-methyl group, and different second nucleosides. Hence, this compensation mechanism can be ruled out. (2) If the range of the observed binding free energies (ΔG°) is small in relation to the binding enthalpy (ΔH°), then the linear correlation results from $\Delta H^\circ - T\Delta S^\circ = \Delta G^\circ \approx$ constant. The ΔG° values of eIF4E−cap association are always greater than 50% of the corresponding ΔH° values (Table 2), so that this case can also be excluded. (3) The last problem is whether enthalpy−entropy compensation is fortuitous resulting from a high correlation between errors of ΔH° and ΔS° obtained by the van't Hoff method. A statistical test has been proposed to determine the significance of the ΔH° vs ΔS° plot observed (*46*). The most exact criterion is to check whether the experimental temperature (T_{exp}) lies outside the 95% confidence interval for the compensation temperature: $T_{exp} < T_c - 2\sigma$ or $T_c + 2\sigma < T_{exp}$. The 95% interval for the cap analogue series is 351−447 K, while the harmonic mean value of the experimental temperatures applied for the van't Hoff analysis is ∼297 K. Hence, the difference between T_c and T_{exp} is even more than 4σ, which unambiguously points to strong, nontrivial, isothermal enthalpy−entropy compensation.

DISCUSSION

Role of Enthalpy and Entropy Changes in eIF4E−Cap Recognition. Thermodynamic analysis of the binding between eIF4E and various chemical cap analogues provides more detailed information on the recognition specificity. The negative enthalpy change at 293 K plays a more pronounced role in binding of the 7-methylated cap analogues with longer phosphate chains, which possess unfavorable entropy. An enthalpy decrease resulting from a comparison of the binding enthalpies for m^{7}GMP and m^{7}GDP equals $\Delta H^\circ_{m7GDP} - \Delta H^\circ_{m7GMP} = -25.9 \pm 8.4$ kJ mol^{-1}, and elongation of the phosphate chain to three groups leads to a further enthalpy decrease of $\Delta H^\circ_{m7GTP} - \Delta H^\circ_{m7GDP} = -12.4 \pm 4.6$ kJ mol^{-1}. These enthalpy differences, when divided by the number of hydrogen bonds or salt bridges formed by the β and γ phosphate groups (2 and 1, respectively, Figure 1), yield almost equal values of the unitary enthalpy change per bond, $\Delta\Delta H^\circ_B \approx -13$ kJ mol^{-1}, which is a typical value for hydrogen bonds (*48*). Although, in general, the binding entropy cannot be theoretically decomposed into individual atom−atom interactions, in this case the entropic penalties, which equal $\Delta S^\circ_{m7GDP} - \Delta S^\circ_{m7GMP} = -61 \pm 11$, and $\Delta S^\circ_{m7GTP} - \Delta S^\circ_{m7GDP} = -30 \pm 16$ J mol^{-1} K^{-1}, appear to yield an average of $\Delta\Delta S^\circ_B \approx -30$ J mol^{-1} K^{-1} per bond. This observation can serve as an indicator that binding of the subsequent phosphate group is approximately independent of binding of the previous group, i.e., there is no measurable entropic effect associated with linkage of the phosphates, arising from a change in the number of degrees of freedom.

The binding entropy at 293 K is more conducive to association of the analogues possessing more or larger substituents in the guanine moiety. For increasingly larger substituents at N(7) in the series of triphosphates 7-methyl-, 7-benzyl-, and 7-*p*-chloro-benzyl-GTP, the binding entropy increases subsequently by +46 ± 18 and +69 ± 20 J mol^{-1} K^{-1}, while the binding enthalpy becomes less negative by +17.8 ± 5.2 and +18 ± 6.0 kJ mol^{-1}, respectively. Consequently, the higher affinity of *p*-Cl-bz^{7}GTP for eIF4E arises from the more favorable entropy change. Several explanations of the strong changes of binding entropy for the cap analogues that differ in substitution at N(7) are plausible. Most likely, the positive entropy change is caused by expulsion of a few water molecules from the depth of the cap-binding slot into the bulk solvent, proportionally to the volume of N(7)-substituent. The large and electronegative chloride atom at the N^7-benzyl ring can attenuate the van der Waals interaction with Trp166 and destroy the specific water network inside the eIF4E cap-binding center due to steric and electrostatic effects (Figure 1). Alternatively, one may try to interpret the changes of the thermodynamic parameters in terms of some changes of the stacking effectivity. More positive entropy and enthalpy of association seem to correlate with more positive values of the Hammett

Table 4: Equilibrium Constants ($_1K$) and Standard Molar Enthalpy Changes ($_1\Delta H°$) for Intramolecular Self-Stacking of the Dinucleotide Cap Analogues. Apparent Contributions to Standard Molar Enthalpy ($\Delta H°_{sst}$), Entropy ($\Delta S°_{sst}$), and Heat Capacity ($\Delta C_p°_{sst}$) Changes of eIF4E Association with Cap Analogues, Resulting from the Shift of the Self-Stacking Equilibrium Induced by Mandatory Coupling of Unstacking to the eIF4E Binding, at 293 K, pH 7.2

cap analogue	$_1K$	$_1\Delta H°$ (kJ mol^{-1})	$\Delta H°_{sst}$ (kJ mol^{-1})	$\Delta S°_{sst}$ (J mol^{-1} K^{-1})	$\Delta C_p°_{sst}$ (J mol^{-1} K^{-1})
m^{7}Gpppp(m^{7}G)[a]	0.32	-15.8 ± 0.7	$+3.85 \pm 0.59$	$+10.81 \pm 1.38$	-64.5 ± 8.3
m^{7}GpppG[b]	1.47	-16.6 ± 0.4	$+9.89 \pm 1.17$	$+30.5 \pm 2.6$	-93.2 ± 10.4
m^{7}GpppC[c]	0.18	-12.0 ± 0.8	$+1.83 \pm 0.44$	$+4.87 \pm 0.82$	-26.1 ± 5.8

[a] Values estimated from the assumptions that $pK_a = 7.2$ for both ends, there is no stacking for the double cationic form, and stacking for the zwitterionic−cationic form is the same as for the double zwitterionic form (pH 9.0 (*31*)). [b] Values calculated from $pK_a = 7.35 \pm 0.05$ (*44*), $_1K$ and $_1\Delta H°$ at pH 5.2 and 9.0 (*31*). [c] $_1K$ and $_1\Delta H°$ assumed to be the same as for the cationic form (pH 5.2 (*31*)).

Table 5: Standard Molar Enthalpy ($\Delta H°_0$), Entropy ($\Delta S°_0$), and Gibbs Free Energy Changes ($\Delta G°_0$), Critical Temperatures T_{H_0} and T_{S_0} (Where $\Delta H°_0 = 0$ and $\Delta S°_0 = 0$, Respectively) and Standard Molar Heat Capacity Changes under Constant Pressure ($\Delta C_p°_0$) for Intrinsic Binding of eIF4E to the Unstacked Dinucleotide Cap Analogues, at 293 K, pH 7.2

cap analogue	$\Delta H°_0$ (kJ mol^{-1})	$\Delta S°_0$ (J mol^{-1} K^{-1})	$\Delta G°_0$ (kJ mol^{-1})	T_{H_0}(K)	T_{S_0}(K)	$\Delta C_p°_0$ (kJ mol^{-1} K^{-1})
m^{7}Gpppp(m^{7}G)[a]	-85 ± 54	-147 ± 88	-42 ± 60	342 ± 35	319.2 ± 18.5	$+1.73 \pm 0.57$
m^{7}GpppG	-75 ± 31	-122 ± 58	-39 ± 35	330 ± 23	311.5 ± 12.5	$+2.01 \pm 0.93$
m^{7}GpppC	-52 ± 28	-50 ± 29	-37 ± 29	310.6 ± 11.8	298.1 ± 3.6	$+2.99 \pm 1.25$

[a] Microscopic association constant has been taken into account.

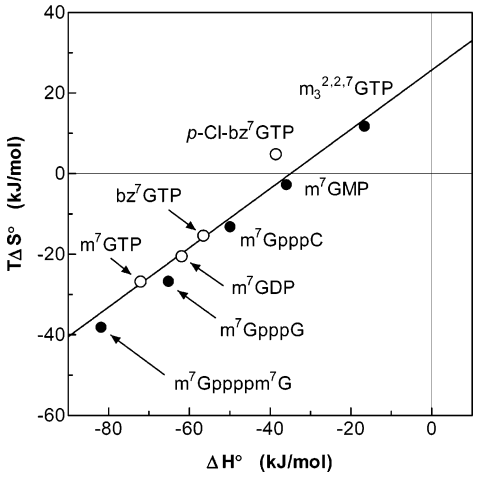

FIGURE 6: Isothermal enthalpy−entropy compensation for the mRNA 5′ cap congener series at 293 K. The enthalpy gain is always greater than the entropy loss that accompanies the association of increasingly more tightly binding cap analogues, irrespective of whether the binding is described by a zero (○) or nonzero (●) heat capacity change. The linear fitting was performed with weighting by errors of both $T\Delta S°$ and $\Delta H°$ (Table 1, the errors not shown for clarity).

constants (σ_p, σ_m) and the difference between them ($\Delta\sigma$) for the larger N(7)-substituents. However, as shown previously for a longer series of cap analogues (*13*), the stacking inside the eIF4E cap-binding slot is only dependent on the presence of any substituent at N(7), which introduces a positive charge in the guanine ring, and not on its type.

In the case of the trimethylated cap analogue, m$_3^{2,2,7}$GTP, the relative contribution of the hydrophobic interactions to $\Delta G°$ at 293 K increases due to fewer hydrogen bonds stabilizing the complex (Figure 1) and much weaker cation−π stacking (*30*) which itself would provide a large enthalpic component, as shown by the NMR measurements. Hence, the thermodynamic driving force for m$_3^{2,2,7}$GTP is more entropic.

The induced shift in the self-stacking equilibrium of the dinucleotide cap analogues significantly contributes to the enthalpy and entropy of the eIF4E−cap association but gives a negligible negative contribution to the overall $\Delta C_p°$. The $\Delta C_p°_{sst}$ values of several tens of J mol^{-1} K^{-1} due to the thermodynamic coupling of cap unstacking to eIF4E binding are close to the results obtained for the coupling of adenine base unstacking to binding with the SSB protein, -62.8 ± 2.5 J mol^{-1} K^{-1} per stack (*49*).

Origins of the Positive Heat Capacity Changes. The majority of the thermodynamic studies report negative values of $\Delta C_p°$ related to specific binding between proteins and nucleic acids (e.g., refs *35*−*39*). Only few results are available on intermolecular interactions that reveal a positive $\Delta C_p°$ value upon complex formation (*50*−*52*). In this context, the molecular origins of our unusual, positive heat capacity changes of +1.66 to +5.12 kJ mol^{-1} K^{-1} (Table 2), confirmed independently by direct microcalorimetric measurements (*14*), need elucidation. Plausible explanations, i.e., surface effects and electrostatic and cation−π stacking contributions, are discussed in the subsequent three sections.

Surface Effects. The $\Delta C_p°$ values are most often dominated by changes of solvent-accessible surfaces upon binding (*35*). The main negative contribution results from a hydrophobic effect, i.e., the removal of a nonpolar and aromatic molecular surface from water, whereas the burial of the polar surface area leads to a ∼2-fold smaller, positive contribution (*53*−*55*). Binding of eIF4E to the cap structure is accompanied by conformational change(s) of the protein and the uptake of ∼65 water molecules by the complex (*13*). On the other hand, cooperativity of the cap-binding site with the eIF4G/4E-BP-binding site (*13*, *56*) suggests that the hydrophobic dorsal surface of eIF4E that is recognized by eIF4G and 4E-BP1 becomes more accessible after the cap has been bound. To estimate the upper limit of the positive contribution to $\Delta C_p°$ from hydration of the hydrophobic surface of the protein, one should take into account only these water molecules that belong to the first-layer hydration shell, and not those trapped inside the cap-binding center (at least 16 water molecules (*13*)), since water in internal cavities is usually stiffly bound (*57*, *58*). Since the surface hydrated by one water molecule is ∼9.5 Å^2 (*59*, *60*), if all remaining water molecules hydrated a purely aliphatic surface of ∼465 Å^2, and if one took the maximal increment of $\Delta C_p°$ per 1 Å of aliphatic surface (+2.14 J mol^{-1} K^{-1}, (*55*)), the calculated

maximum possible contribution to $\Delta C_p°$ from hydrophobic effects would then equal about +1 kJ mol^{-1} K^{-1}.

Heat capacity changes for the burial of nucleic acid components were calculated recently as +52.63 J mol^{-1} K^{-1} for guanine, −36.07 J mol^{-1} K^{-1} for ribose, and +46.02 J mol^{-1} K^{-1} for a single phosphate group (*61*). Neglecting neighbor effects between base, sugar, and phosphate groups in the complete cap analogue, and the unknown resultant influence of guanosine methylation that provides both the additional aliphatic group and the positive charge to the ring, the estimated range of contribution from the burial of 7-methylguanosine triphosphate would equal about +0.2 kJ mol^{-1} K^{-1}.

Electrostatic Contributions to Heat Capacity Changes. Area-based models of the heat capacity changes take into account short-range effects related to energy fluctuations of water imposed by the macromolecular surface. There are three direct electrostatic contributions to $\Delta C_p°$ upon binding, which do not scale with the surface area (*62*): the rearrangement of water dipoles, the redistribution of mobile ions in the solvent, and the coupling between the dipolar and ionic terms. The overall electrostatic contribution to $\Delta C_p°$ due to dehydration of charged residues is dominated by the positive term arising from the dielectric behavior of water. Therefore, changes in the solution structure can also partially account for the observed positive $\Delta C_p°$. However, the possible electrostatic contribution from the phosphate groups of the cap analogues and the basic amino acid side chains in the protein cap-binding site is 1 order of magnitude lower than that arising from the surface effects (*62*).

Thermodynamics of Cation−π Stacking. The $\Delta H°$ values for stacking of the 7-methylG moiety with tryptophan are ∼2-fold greater (Table 3) than those reported for adenine and uracil base stacking, −12.6 to −14.2 kJ mol^{-1} per stack (*40*, *49*, *63*), and for intramolecular self-stacking of the dinucleotide cap analogues ($_1\Delta H°$, Table 4). The enthalpy and entropy changes of the m^{7}G-Trp stacking provide a significant contribution to the overall thermodynamic parameters of cap binding to eIF4E upon translation initiation. The 7-methylG moiety represents a unique example of a cation that is concurrently a heteroaromatic ring. The large, negative values of both $\Delta H°$ and $\Delta S°$ for stacking of 7-methylG with tryptophan come from the Coulombic character of the cation−π interactions. As opposed to regular π−π stacking in single stranded nucleic acids (*40*, *41*), the 7-methylguanine sandwich stacking between Trp102 and Trp56 within the cap-binding site of eIF4E can provide a substantial positive contribution to $\Delta C_p°$.

Many proteins recognize specifically nucleic acid ligands by π−π stacking between a nucleobase and aromatic amino acid side chains. Two proteins involved in mRNA metabolism have been proved to associate with mRNA 5′ cap by cation−π stacking, i.e., mammalian eIF4E (*13*, *14*) and VP39, viral mRNA cap-specific 2′-O-methyltranferase (*64*). The crystal structure of human CBC in complex with m^7-GpppG (*65*) suggests also binding of the cationic form of the 7-methylguanine moiety. It can be expected that proteins which interact with the cationic nucleobase can have thermodynamic features similar to those of eIF4E, contrary to other cap-binding proteins, interacting by π−π stacking with nonmethylated G, e.g., viral and yeast guanine-7-methyltransferases (*66*, *67*).

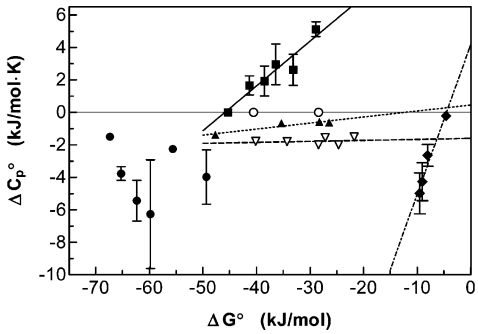

FIGURE 7: Correlation of heat capacity changes ($\Delta C_p°$) with standard molar binding free energies ($\Delta G°$) for different intermolecular interactions: eIF4E with mRNA 5′ cap analogues (■); DNA with intercalators (▲); L-isoleucine tRNA ligase with substrates (▽); serine proteases with Na^+ (◆); specific protein binding to DNA (●); nonspecific protein binding to DNA (○).

In summary, the results presented combined with the literature data allow us to conclude that the hydration of the eIF4E hydrophobic dorsal surface, cation−π stacking, and the burial of other ionized and uncharged polar surfaces of the cap analogue and the protein binding site can together yield the positive $\Delta C_p°$ at the level of a few kJ mol^{-1} K^{-1} upon cap binding.

Linear Correlation between $\Delta C_p°$ and $\Delta G°$. Figure 7 shows that the values of $\Delta C_p°$ correlate linearly (correlation coefficient $r^2 = 0.91$) with the free energies of complex stabilization: the stronger the binding, the less positive is the $\Delta C_p°$ value. The cap analogues with the highest binding affinity, e.g., 7-methylGTP, do not reveal any observable curvature of the van't Hoff plot (Figure 3). Systematic $\Delta C_p°$ dependence on the cap affinity for eIF4E suggests, independently of the above-mentioned isothermal enthalpy−entropy compensation, that the positive contribution is compensated to different extents by the negative contribution related to the tightening of the global fold of the protein upon binding (*35*). It was shown (*32*) that preferential ligand binding to the lower microstates of a protein lead to a shift in the distribution of the microstates, and consequently, the reduced width of the distribution implies a decrease in heat capacity upon ligand binding. A salient example of a strong, negative stabilization effect of $\Delta C_p° \sim -1.6$ kJ mol^{-1} K^{-1}, which was completely unrelated to the hydrophobic surface effects, was reported for specific antigen−antibody association (*68*).

A linear $\Delta G°$ vs $\Delta C_p°$ correlation is rarely found, since it requires systematic studies on a consistent ligand series, while suitable data obtained by time- and protein-consuming thermodynamic measurements are rather scattered. The examples available are assembled in Figure 7. A general tendency is common, but only two processes involving charged ligands, i.e., specific sodium cation binding by serine proteases (*69*) and eIF4E−cap binding, yield remarkable slopes (0.93 ± 0.14 K^{-1} and 0.275 ± 0.044 K^{-1}, respectively). In contrast, binding of the L-isoleucine tRNA ligase to its various substrates, which is not accompanied by any conformational changes of this large (120 kDa), multidomain protein (*70*), is accompanied by approximately equal heat capacity changes, although the range of the corresponding free energy changes covers almost 20 kJ mol^{-1} (*71*). Drug−DNA intercalation is related partially to the binding-induced changes in nonpolar and polar solvent-accessible surface areas, and consequently the binding free energy is slightly

proportional to the hydrophobic effect (*72*−*74*). Specific interactions of DNA with repressors and RNA polymerase, driven by hydrophobicity of the specific sites, are characterized by widespread protein conformational changes and large negative heat capacity changes (*37*), while nonspecific interactions, driven only by entropic counterion release, are accomplished with $\Delta C_p^\circ = 0$ (*75*). Searching for the origins of the positive ΔC_p° and for the causal explanation of the linear relationship in terms of statistical physics should be the subject of further investigations.

Molecular Interpretation of Isothermal Enthalpy−*Entropy Compensation.* Enthalpy−entropy compensation was described in terms of statistical mechanics by a compensation temperature (T_c) shown to be related to the difference between the mean energy (E°) of an unperturbed system (e.g., the *apo*-protein) and the energy ($U^{\circ\prime}$) of a significantly perturbed state (e.g., the protein microstate interacting with a ligand) (*47*):

$$T_c = \frac{\Delta H^\circ}{\Delta S^\circ} \approx \frac{\Delta E^\circ}{\Delta S^\circ} \approx \frac{T}{1 - \frac{RT}{E^\circ - U^{\circ\prime}}} \qquad (19)$$

However, no clear interpretation for the T_c value was proposed. It seems that the difference between the compensation temperature and the harmonic mean experimental temperature can be a measure of the fluctuations of the unperturbed system, which are modulated by the perturbation. Depending on whether T_c is greater or lower than T_{exp}, the fluctuations are either silenced or enhanced, and therefore the perturbation acts in either a stabilizing or destabilizing manner, respectively. Thus, the T_c value of 399 ± 24 K shows that the energy ($U^{\circ\prime}$) of the state of eIF4E which binds to the cap structure lies much below the mean energy of the *apo*-protein (E°): $E^\circ - U^{\circ\prime} = 9.66 \pm 1.7$ kJ mol^{-1}. This large energy difference, far exceeding *RT* (∼2.5 kJ mol^{-1} at 300 K), and almost comparable with the stabilization energy of globular proteins of similar size and hydrophobicity (∼50 kJ mol^{-1}) (*76*), suggests that the *apo*-eIF4E is a highly fluctuating protein, and only the specific cap binding provides enough stiffening of the functional protein structure.

One difficulty in interpretation is related to the lack of the crystal structure of *apo*-eIF4E which is indispensable for the complete analysis. The thermodynamic results, however, can lead to well-grounded predictions of a putative role of the eIF4E structural flexibility in translation initiation. The two-step molecular mechanism of the mRNA 5′ cap binding (*12*, *13*) lies in anchoring of the cap through the phosphate chain and subsequent formation of the cation−π sandwich of 7-methylguanine between two tryptophans (Trp102, Trp56) together with hydrogen bonds of the 7-methylguanine moiety (*13*) (Figure 1). High fluctuations of the *apo*-eIF4E suggest an "open" form of the *apo*-protein, in which two loops containing Trp102 and Trp56 (Figure 1) are far aside from each other, and become more ordered and stiffened only after cap binding.

Significant conformational changes of eIF4E upon association with cap implicated by the large energy difference ($E^\circ - U^{\circ\prime}$) could also modify the dorsal part of eIF4E that gets into contact with eIF4G or 4E-BPs (*77*) and thus can account for cooperativity of the two eIF4E binding centers (*13*, *56*, *78*). Hence, the isothermal enthalpy−entropy compensation elucidates some basic biological properties of eIF4E that are key to its cellular role.

Biological Implications of Nonlinear van't Hoff Thermodynamics. Unique thermodynamic features of the eIF4E−cap system provide a better understanding of the complicated process of protein−nucleic acid recognition and can shed some light on in vivo metabolic pathways. The nonzero heat capacity changes for the two natural dinucleotide cap analogues have the following impact at biological temperatures (∼310 K). (1) Recognition of the cap by eIF4E is both enthalpy and entropy favorable. (2) The affinities of eIF4E for the 5′ caps containing G or C as first transcribed nucleoside are almost equal. (3) Stabilization of these complexes is relatively temperature-invariant, contrary to binding of eIF4E to the translation initiation inhibitor, 4E-BP1, which is increased by heat shock (*79*−*81*).

The results obtained for the mononucleotide triphosphates show that thermodynamic driving forces distinguish between the MMG cap (m^{7}GTP) and the TMG cap (m$_3^{2,2,7}$GTP) within the biological temperature range. The association constant of m^{7}GTP is ∼110-fold greater than that of m$_3^{2,2,7}$-GTP at 310 K (37 °C). Due to the positive heat capacity change, the m$_3^{2,2,7}$GTP binding enthalpy at 310 K attains the same absolute value of $\Delta H^\circ_{310K} = +69.6 \pm 6.9$ kJ mol^{-1} as that for m^{7}GTP (Table 1) but with the opposite sign, although both analogues have charged triphosphate chains. Hence, an increase in temperature in this range enhances affinity of eIF4E for m$_3^{2,2,7}$GTP and reduces affinity for m^{7}GTP. This phenomenon diminishes the predominance of m^{7}GTP affinity in relation to m$_3^{2,2,7}$GTP to ∼57-fold already at 313 K (40 °C). The distinct thermodynamic parameters of m^{7}GTP and m$_3^{2,2,7}$GTP could thus influence to some extent the biochemical equilibria related to splicing, protein biosynthesis, and relations between one another in eukaryotic cells during heat shock.

In some primitive eukaryotes (*82*−*84*) and in some chordate species (*85*) the process of trans-splicing leads mRNAs to contain the TMG cap structure. In even ∼70% of the mRNA population in the *Caenorhabditis elegans* nematode, the original cap is replaced by m$_3^{2,2,7}$GpppN. Five eIF4E-like translation initiation factors (IFEs) with the sequence identity to human eIF4E of 30−47% were found in this organism (*86*). The tertiary structures and the cellular role for the individual eIF4E isoforms are still unknown, although some of them are essential for viability of the worm embryos (*86*). Three of the IFEs bind to both m^{7}GTP and m$_3^{2,2,7}$GTP (*86*−*88*). The mechanism of discrimination between MMG and TMG caps is unclear. Extension of thermodynamic analysis on the eIF4E isoforms from *C. elegans* will provide clues for differences in the cap structure discrimination among the IFE proteins observed in biological assays (*86*). Due to small structural differences expected for the IFE proteins possessing high amino acid identity, we foresee that this mechanism of discrimination could be based rather on the dynamic structural fluctuations of the proteins (see enthalpy−entropy compensation).

CONCLUSIONS

The thermodynamic studies presented here reveal the unique, large and positive heat capacity changes at constant pressure that accompany interactions between eIF4E and the

mRNA 5′ cap. The positive sign of the ΔC_p° values appears to be a characteristic feature of eIF4E binding to the cap. The ΔC_p° values at the level of a few kJ mol^{-1} K^{-1} can be attributed to simultaneous interplay of various intermolecular processes upon cap−eIF4E complex formation, such as the additional hydration of the eIF4E hydrophobic dorsal surface, cation−π stacking, and the burial of other ionized and uncharged polar surfaces of the cap analogue and the protein binding site, as well as nonmandatory coupling (*32*) with partial protonation of cap, water uptake, and conformational changes of the protein (*13*, *14*).

The chemical cap analogues of the highest specificity for eIF4E have the heat capacity change proportionally shifted toward less positive or undetectable values. The negative contribution canceling the positive contribution for the most tightly binding cap analogues arises from significant protein stiffening in the complex structure, as implied from the high value of the characteristic temperature (399 ± 24 K) of the exceptional, nontrivial and statistically important isothermal enthalpy−entropy compensation. True, extrathermodynamic compensation reflects thermodynamic features of the macromolecular system, the dominating enthalpic character for the entire congener series, a great flexibility of the *apo*-form of eIF4E, and stiffening of eIF4E in the cap-bound state.

The results presented contribute to more profound insights into how eIF4E interacts with other components of the cytoplasmic machinery responsible for cap-dependent translation initiation. The thermodynamic properties of the mRNA 5′ cap interactions with eIF4E described here in terms of biophysics shed light on some intermolecular equilibria in the eukaryotic cell and are also a type of challenge for theoretical interpretation.

ACKNOWLEDGMENT

We thank Dr. Janusz Stepinski and Dr. Marzena Jankowska-Anyszka for providing the cap analogues, Prof. Nahum Sonenberg for the eIF4E plasmid, Lilia Zhukova for the eIF4E expression and purification, and Prof. Anne-Lise Haenni and Prof. Marek Cieplak for critical reading of the manuscript.

REFERENCES

1. Varani, G. (1997) A cap for all occasions, *Structure 5*, 855−858.
2. Furuichi, Y., and Shatkin, A. J. (2000) Viral and cellular mRNA capping: Past and prospects, *Adv. Virus Res. 55*, 135−184.
3. Mattaj, I. W. (1986) Cap trimethylation of U snRNA is cytoplasmic and dependent on U snRNP protein binding, *Cell 46*, 905−911.
4. Hamm, J., Darzynkiewicz, E., Tahara, S. M., and Mattaj, I. W. (1990) The trimethylguanosine cap structure of U1 snRNA is a component of a bipartite nuclear targeting signal, *Cell 62*, 569−577.
5. Gorlich, D., and Mattaj, I. W. (1996) Nucleocytoplasmic transport, *Science 271*, 1513−1518.
6. Sharp, P. A. (1994) Split genes and RNA splicing, *Cell 77*, 805−815.
7. Sonenberg, N., Morgan, M. A., Merrick, W. C., and Shatkin, A. J. (1978) A polypeptide in eukaryotic initiation factors that crosslinks specifically to the 5′-terminal cap in mRNA, *Proc. Natl. Acad. Sci. U.S.A. 75*, 4843−4847.
8. Izaurralde, E., Lewis, J., McGuigan, C., Jankowska, M., Darzynkiewicz, E., and Mattaj, I. W. (1994) A nuclear cap binding protein complex involved in pre-mRNA splicing, *Cell 78*, 657−668.
9. Raught, B., and Gingras, A. C. (1999) eIF4E activity is regulated at multiple levels, *Int. J. Biochem. Cell Biol. 31*, 43−57.
10. Marcotrigiano, J., Gingras, A. C., Sonenberg, N., and Burley, S. K. (1997) Cocrystal structure of the messenger RNA 5′ cap-binding protein (eIF4E) bound to 7-methyl-GDP, *Cell 89*, 951−961.
11. Matsuo, H., Li, H., McGuire, A. M., Fletcher, C. M., Gingras, A. C., Sonenberg, N., and Wagner, G. (1997) Structure of translation factor eIF4E bound to m7GDP and interaction with 4E-binding protein, *Nat. Struct. Biol. 4*, 717−724,
12. Blachut-Okrasinska, E., Bojarska, E., Niedzwiecka, A., Chlebicka, L., Darzynkiewicz, E., Stolarski, R., Stepinski, J., and Antosiewicz, J. M. (2000) Stopped-flow and Brownian dynamics studies of electrostatic effects in the kinetics of binding of 7-methyl-GpppG to the protein eIF4E, *Eur. Biophys. J. 29*, 487−498.
13. Niedzwiecka, A., Marcotrigiano, J., Stepinski, J., Jankowska-Anyszka, M., Wyslouch-Cieszynska, A., Dadlez, M., Gingras, A. C., Mak, P., Darzynkiewicz, E., Sonenberg, N., Burley, S. K., and Stolarski, R. (2002) Biophysical studies of eIF4E cap-binding protein: recognition of mRNA 5′ cap structure and synthetic fragments of eIF4G and 4E-BP1 proteins, *J. Mol. Biol. 319*, 615−635.
14. Niedzwiecka, A., Stepinski, J., Darzynkiewicz, E., Sonenberg, N., and Stolarski, R. (2002) Positive heat capacity change upon specific binding of translation initiation factor eIF4E to mRNA 5′ cap, *Biochemistry 41*, 12140−12148.
15. Tomoo, K., Shen, X., Okabe, K., Nozoe, Y., Fukuhara, S., Morino, S., Ishida, T., Taniguchi, T., Hasegawa, H., Terashima, A., Sasaki, M., Katsuya, Y., Kitamura, K., Miyoshi, H., Ishikawa, M., and Miura, K. (2002) Crystal structures of 7-methylguanosine 5′-triphosphate (m(7)GTP)- and P(1)-7-methylguanosine-P(3)-adenosine-5′, 5′-triphosphate (m(7)GpppA)-bound human full-length eukaryotic initiation factor 4E: biological importance of the C-terminal flexible region, *Biochem. J. 362*, 539−544.
16. Zuberek, J., Wyslouch-Cieszynska, A., Niedzwiecka, A., Dadlez, M., Stepinski, J., Augustyniak, W., Gingras, A. C., Zhang, Z., Burley, S. K., Sonenberg, N., Stolarski, R., and Darzynkiewicz, E. (2003) Phosphorylation of eIF4E attenuates its interaction with mRNA 5′ cap analogs by electrostatic repulsion: Intein-mediated protein ligation strategy to obtain phosphorylated protein, *RNA 9*, 52−61.
17. Sonenberg, N. (1996) mRNA 5′ cap-binding protein eIF4E and control of cell growth, in *Translational Control* (Hershey, J. W. B., Mathews, M. B.,and Sonenberg, N., Eds.) pp 245−269, Cold Spring Harbor Laboratory Press, New York.
18. Gingras, A. C., Raught, B., and Sonenberg, N. (1999) eIF4 initiation factors: effectors of mRNA recruitment to ribosomes and regulators of translation, *Annu. Rev. Biochem. 68*, 913−963.
19. Raught, B., Gingras, A. C., and Sonenberg, N. (2000) Regulation of ribosomal recruitment in eukaryotes, in *Translational Control of Gene Expression* (Sonenberg, N., Hershey, J. W., and Mathews, M. B.) pp 245−293, Cold Spring Harbor Laboratory Press, New York.
20. Duncan, R., Milburn, S. C., and Hershey, J. W. (1987) Regulated phosphorylation and low abundance of HeLa cell initiation factor eIF-4F suggest a role in translational control. Heat shock effects on eIF-4F, *J. Biol. Chem. 262*, 380−388.
21. Hershey, J. W., and Miyamoto, S. (2000) Translational control and cancer, in *Translational Control of Gene Expression* (Sonenberg, N,, Hershey, J. W., and Mathews, M. B., Eds.) pp 637−654, Cold Spring Harbor Laboratory Press, New York.
22. De Benedetti, A., and Harris, A. L. (1999) eIF4E expression in tumors: its possible role in progression of malignancies, *Int. J. Biochem. Cell Biol. 31*, 59−72.
23. Darzynkiewicz, E., Ekiel, I., Tahara, S. M., Seliger, L. S., and Shatkin, A. J. (1985) Chemical synthesis and characterization of 7-methylguanosine cap analogues, *Biochemistry 24*, 1701−1707.
24. Edery, I., Altmann, M., and Sonenberg, N. (1988) High-level synthesis in Escherichia coli of functional cap-binding eukaryotic initiation factor eIF-4E and affinity purification using a simplified cap-analog resin, *Gene 74*, 517−525.
25. Cai, A., Jankowska-Anyszka, M., Centers, A., Chlebicka, L., Stepinski, J., Stolarski, R., Darzynkiewicz, E., and Rhoads, R. E. (1999) Quantitative assessment of mRNA cap analogues as inhibitors of in vitro translation, *Biochemistry 38*, 8538−8547.
26. Parker, C. A. *Photoluminescence of Solutions*, Elsevier Publishing Company, Amsterdam.
27. Baldwin, R. L. (1986) Temperature dependence of the hydrophobic interaction in protein folding, *Proc. Natl. Acad. Sci. U.S.A. 83*, 8069−8072.

28. Hore, P. J. (1983) Solvent suppression in Fourier transform nuclear magnetic resonance, *J. Magn. Reson. 55*, 283−300.
29. Brown, L. R.; Farmer, B. T. (1989) Rotating-frame nuclear Overhauser effect, *Methods Enzymol. 176*, 199−216.
30. Stolarski, R., Sitek, A., Stepinski, J., Jankowska, M., Oksman, P., Temeriusz, A., Darzynkiewicz, E., Lonnberg, H., and Shugar, D. (1996) 1H-NMR studies on association of mRNA cap-analogues with tryptophan-containing peptides, *Biochim. Biophys. Acta 1293*, 97−105.
31. Wieczorek, Z., Zdanowski, K., Chlebicka, L., Stepinski, J., Jankowska, M., Kierdaszuk, B., Temeriusz, A., Darzynkiewicz, E., and Stolarski, R. (1997) Fluorescence and NMR studies of intramolecular stacking of mRNA cap-analogues, *Biochim. Biophys. Acta 1354*, 145−152.
32. Eftink, M. R., Anusiem, A. C., and Biltonen, R. L. (1983) Enthalpy−entropy compensation and heat capacity changes for protein−ligand interactions: general thermodynamic models and data for the binding of nucleotides to ribonuclease A, *Biochemistry 22*, 3884−3896.
33. Beyer, W. H. (1987) *CRC Standard mathematical tables*, CRC Press, Boca Raton, FL.
34. Taylor, J. R. (1982) *An introduction to error analysis*, University Science Books, Mill Valley, CA.
35. Sturtevant, J. M. (1977) Heat capacity and entropy changes in processes involving proteins, *Proc. Natl. Acad. Sci. U.S.A. 74*, 2236−2240.
36. Spolar, R. S., Ha, J. H., and Record, M. T., Jr. (1989) Hydrophobic effect in protein folding and other noncovalent processes involving proteins, *Proc. Natl. Acad. Sci. U.S.A. 86*, 8382−8385.
37. Ha, J. H., Spolar, R. S., and Record, M. T., Jr. (1989) Role of the hydrophobic effect in stability of site-specific protein-DNA complexes, *J. Mol. Biol. 209*, 801−816.
38. Spolar, R. S., and Record, M. T., Jr. (1994) Coupling of local folding to site-specific binding of proteins to DNA, *Science 263*, 777−784.
39. Patikoglou, G., and Burley, S. K. (1997) Eukaryotic transcription factor-DNA complexes, *Annu. Rev. Biophys. Biomol. Struct. 26*, 289−325.
40. Filimonov, V. V., and Privalov, P. L. (1978) Thermodynamics of base interaction in (A)n and (A.U)n, *J. Mol. Biol. 122*, 465−470.
41. Holbrook, J. A., Capp, M. W., Saecker, R. M., and Record, M. T. (1999) Enthalpy and heat capacity changes for formation of an oligomeric DNA duplex: Interpretation in terms of coupled processes of formation and association of single-stranded helices, *Biochemistry 38*, 8409−8422.
42. Dougherty, D. A. (1996) Cation-pi interactions in chemistry and biology: a new view of benzene, Phe, Tyr, and Trp, *Science 271*, 163−168.
43. Niedzwiecka-Kornas, A., Przedmojski, R., Balaspiri, L., Wieczorek, Z., Stepinski, J., Jankowska, M., Lonnberg, H., Darzynkiewicz, E., and Stolarski, R. (1999) Studies on association of mRNA cap-analogues with a synthetic dodecapeptide DGIEPMWEDEKN, *Nucleosides Nucleotides 18*, 1105−1106.
44. Wieczorek, Z., Stepinski, J., Jankowska, M., and Lonnberg, H. (1995) Fluorescence and absorption spectroscopic properties of RNA 5′-cap analogues derived from 7-methyl-, N2,7-dimethyl- and N2,N2,7-trimethyl-guanosines, *J. Photochem. Photobiol. B 28*, 57−63.
45. Lumry, R., and Rajender, S. (1970) Enthalpy-entropy compensation phenomena in water solutions of proteins and small molecules: a ubiquitous property of water, *Biopolymers 9*, 1125−1227.
46. Krug, R. R., Hunter, W. G., and Grieger, R. A. (1976) Statistical interpretation of enthalpy-entropy compensation. *Nature 261*, 566−567.
47. Sharp, K. (2001) Entropy-enthalpy compensation: fact or artifact? *Protein Sci. 10*, 661−667.
48. Pimentel, G. C., and McClellan, A. L. (1971) Hydrogen bonding, *Annu. Rev. Phys. Chem. 22*, 347−385.
49. Kozlov, A. G., and Lohman, T. M. (1999) Adenine base unstacking dominates the observed enthalpy and heat capacity changes for the *Escherichia coli* SSB tetramer binding to single-stranded oligoadenylates. *Biochemistry 38*, 7388−7397.
50. Luther, M. A., Cai, G. Z., and Lee, J. C. (1986) Thermodynamics of dimer and tetramer formations in rabbit muscle phosphofructokinase, *Biochemistry 25*, 7931−7937.
51. Hileman, R. E., Jennings, R. N., and Linhardt, R. J. (1998) Thermodynamic analysis of the heparin interaction with a basic cyclic peptide using isothermal titration calorimetry, *Biochemistry 37*, 15231−15237.
52. Matulis, D., Rouzina, I., and Bloomfield, V. A. (2000) Thermodynamics of DNA binding and condensation: isothermal titration calorimetry and electrostatic mechanism, *J. Mol. Biol. 296*, 1053−1063.
53. Spolar, R. S., Livingstone, J. R., and Record, M. T., Jr. (1992) Use of liquid hydrocarbon and amide transfer data to estimate contributions to thermodynamic functions of protein folding from the removal of nonpolar and polar surface from water, *Biochemistry 31*, 3947−3955.
54. Murphy, K. P., Bhakuni, V., Xie, D., and Freire, E. (1992) Molecular basis of co-operativity in protein folding. III. Structural identification of cooperative folding units and folding intermediates, *J. Mol. Biol. 227*, 293−306.
55. Makhatadze, G. I., and Privalov, P. L. (1995) Energetics of protein structure. *Adv. Protein Chem. 47*, 307−425.
56. Miyoshi, H., Youtani, T., Ide, H., Hori, H., Okamoto, K., Ishikawa, M., Wakiyama, M., Nishino, T., Ishida, T., and Miura, K. (1999) Binding analysis of Xenopus laevis translation initiation factor 4E (eIF4E) in initiation complex formation, *J. Biochem. (Tokyo) 126*, 897−904.
57. Lucke, C., Huang, S., Rademacher, M., and Ruterjans, H. (2002) New insights into intracellular lipid binding proteins: The role of buried water, *Protein Sci. 11*, 2382−2392.
58. Takano, K., Funahashi, J., Yamagata, Y., Fujii, S., and Yutani, K. (1997) Contribution of water molecules in the interior of a protein to the conformational stability, *J. Mol. Biol. 274*, 132−142.
59. Parsegian, V. A., Rand, R. P., and Rau, D. C. (1995) Macromolecules and water: probing with osmotic stress, *Methods Enzymol. 259*, 43−94.
60. Colombo, M. F., Rau, D. C., and Parsegian, V. A. (1992) Protein solvation in allosteric regulation: a water effect on hemoglobin, *Science 256*, 655−659.
61. Madan, B., and Sharp, K. A. (2001) Hydration heat capacity of nucleic acid constituents determined from the random network model, *Biophys. J. 81*, 1881−1887.
62. Gallagher, K., and Sharp, K. (1998) Electrostatic contributions to heat capacity changes of DNA-ligand binding, *Biophys. J. 75*, 769−776.
63. Breslauer, K. J., and Sturtevant, J. M. (1977) A calorimetric investigation of single stranded base stacking in the ribooligonucleotide A7, *Biophys. Chem. 7*, 205−209.
64. Hu, G. H., Tsai, A. L., and Quiocho, F. A. (2003) Insertion of an N7-methylguanine mRNA cap between two coplanar aromatic residues of a cap-binding protein is fast and selective for a positively charged cap, *J. Biol. Chem. 278*, 51515−51520.
65. Mazza, C., Ohno, M., Segref, A., Mattaj, I. W., and Cusack, S. (2001) Crystal structure of the human nuclear cap binding complex, *Mol. Cell 8*, 383−396.
66. Mao, X., and Shuman, S. (1996) Vaccinia virus mRNA (guanine-7-)methyltransferase: Mutational effects on cap methylation and AdoHcy-dependent photo-cross-linking of the cap to the methyl acceptor site, *Biochemistry 35*, 6900−6910.
67. Wang, S. P., and Shuman, S. (1997) Structure-function analysis of the mRNA cap methyltransferase of Saccharomyces cerevisiae, *J. Biol. Chem. 272*, 14683−14689.
68. Bhat, T. N., Bentley, G. A., Boulot, G., Greene, M. I., Tello, D., Dall'Acqua, W., Souchon, H., Schwarz, F. P., Mariuzza, R. A., and Poljak, R. J. (1994) Bound water molecules and conformational stabilization help mediate an antigen−antibody association, *Proc. Natl. Acad. Sci. U.S.A. 91*, 1089−1093.
69. Griffon, N., and Di Stasio, E. (2001) Thermodynamics of Na+ binding to coagulation serine proteases, *Biophys. Chem. 90*, 89−96.
70. Nureki, O., Vassylyev, D. G., Tateno, M., Shimada, A., Nakama, T., Fukai, S., Konno, M., Hendrickson, T. L., Schimmel, P., and Yokoyama, S. (1998) Enzyme structure with two catalytic sites for double-sieve selection of substrate, *Science 280*, 578−582.
71. Hinz, H. J., Weber, K., Flossdorf, J., and Kula, M. R. (1976) Thermodynamic studies on the specificity of L-isoleucine-tRNA ligase of Escherichia coli MRE 600. Calorimetric investigations on binding of amino acids and isoleucinol to the enzyme, *Eur. J. Biochem. 71*, 437−442.
72. Chaires, J. B., Satyanarayana, S., Suh, D., Fokt, I., Przewloka, T., and Priebe, W. (1996) Parsing the free energy of anthracycline antibiotic binding to DNA, *Biochemistry 35*, 2047−2053.

73. Ren, J., Jenkins, T. C., and Chaires, J. B. (2000) Energetics of DNA intercalation reactions, *Biochemistry 39*, 8439−8447.
74. Qu, X., and Chaires, J. B. (2001) Hydration Changes for DNA Intercalation Reactions, *J. Am. Chem. Soc. 123*, 1−7.
75. DeHaseth, P. L., Lohman, T. M., and Record, M. T., Jr. (1977) Nonspecific interaction of lac repressor with DNA: an association reaction driven by counterion release, *Biochemistry 16*, 4783−4790.
76. Creighton, T. E. (1993) *Proteins: structures and molecular properties*, W. H. Freeman and Co., New York.
77. Marcotrigiano, J., Gingras, A. C., Sonenberg, N., and Burley, S. K. (1999) Cap-dependent translation initiation in eukaryotes is regulated by a molecular mimic of eIF4G, *Mol. Cell 3*, 707−716.
78. von der Haar, T., Ball, P. D., and McCarthy, J. E. (2000) Stabilization of eukaryotic initiation factor 4E binding to the mRNA 5′-Cap by domains of eIF4G, *J. Biol. Chem. 275*, 30551−30555.
79. Vries, R. G., Flynn, A., Patel, J. C., Wang, X., Denton, R. M., and Proud, C. G. (1997) Heat shock increases the association of binding protein-1 with initiation factor 4E. *J. Biol. Chem. 272*, 32779−32784.
80. Panniers, R., Stewart, E. B., Merrick, W. C., and Henshaw, E. C. (1985) Mechanism of inhibition of polypeptide chain initiation in heat-shocked Ehrlich cells involves reduction of eukaryotic initiation factor 4F activity, *J. Biol. Chem. 260*, 9648−9653.
81. Lamphear, B. J., and Panniers, R. (1991) Heat shock impairs the interaction of cap-binding protein complex with 5′ mRNA cap, *J. Biol. Chem. 266*, 2789−2794.
82. Zorio, D. A., Cheng, N. N., Blumenthal, T., and Spieth, J. (1994) Operons as a common form of chromosomal organization in C. elegans, *Nature 372*, 270−272.
83. Blumenthal, T., and Steward, K. (1997) in *C. Elegans II* (Riddle, D. L., Blumenthal, T.,Meyer, B. J., and Priess, J. R., Eds.) pp 117−145, Cold Spring Harbor Laboratory, Cold Spring Harbor, NY.
84. Van Doren, K., and Hirsh, D. (1990) mRNAs that mature through trans-splicing in Caenorhabditis elegans have a trimethylguanosine cap at their 5′ termini, *Mol. Cell Biol. 10*, 1769−1772.
85. Vandenberghe, A. E., Meedel, T. H., and. Hastings, K. E (2001) mRNA 5′-leader trans-splicing in the chordates, *Genes Dev. 15*, 294−303.
86. Keiper, B. D., Lamphear, B. J., Deshpande, A. M., Jankowska-Anyszka, M., Aamodt, E. J., Blumenthal, T., and Rhoads, R. E. (2000) Functional characterization of five eIF4E isoforms in Caenorhabditis elegans, *J. Biol. Chem. 275*, 10590−10596.
87. Jankowska-Anyszka, M., Lamphear, B. J., Aamodt, E. J., Harrington, T., Darzynkiewicz, E., Stolarski, R., and Rhoads, R. E. (1998) Multiple isoforms of eukaryotic protein synthesis initiation factor 4E in Caenorhabditis elegans can distinguish between mono- and trimethylated mRNA cap structures, *J. Biol. Chem. 273*, 10538−10542.
88. Stachelska, A., Wieczorek, Z., Ruszczynska, K., Stolarski, R., Pietrzak, M., Lamphear, B. J., Rhoads, R. E., Darzynkiewicz, E., and Jankowska-Anyszka, M. (2002) Interaction of three Caenorhabditis elegans isoforms of translation initiation factor eIF4E with mono- and trimethylated mRNA 5′ cap analogues. *Acta Biochim. Pol. 49*, 671−682.
89. Dawson, R. M., Elliott, D. C., Elliott, W. H., and Jones, K. M. (1969) *Data for biochemical research*, pp 174−175. Clarendon Press, Oxford.

BI0491651